Mem. S.A.It. Vol. 90, 359

Memorie della

The mass-ratio distribution of spectroscopic binaries along the main sequence

H. M. J. Boffin[1] and D. Pourbaix[2]

[1] European Southern Observatory, Karl-Schwarzschild-str. 2, 85748 Garching, Germany
e-mail: hboffin@eso.org
[2] Institut d'Astronomie et d'Astrophysique, Université Libre de Bruxelles, Boulevard du Triomphe, 1050 Bruxelles, Belgium

Abstract. Binarity is now a well-established quality affecting a large fraction of stars, and recent studies have shown that the fraction of binaries is a function of the spectral type of the primary star, with most massive stars being member of a close binary system. By cross-matching the *Gaia* DR2 catalogue with a catalogue of known spectroscopic orbits, we went one step further and derived the mass ratio distribution of binary systems as a function of the spectral type of the primary star, i.e. of its mass. A clear correlation is found, with B stars showing an excess of low-mass companions and A stars showing an excess of twins.

Key words. Stars: binaries – Spectroscopic orbits

1. Introduction

A large fraction of stars are members of binary and multiple systems. The binary frequency of stars has been studied across the whole range of masses, with a lower frequency among M dwarfs and a much higher one among massive stars (Duchêne & Kraus 2013). Thus, for M dwarfs the binary fraction is about 0.25–0.40 (Raghavan et al. 2010; Ward-Duong et al. 2015). For solar-like stars, the ratio is around 0.45–0.6 (Duquennoy & Mayor 1991; Raghavan et al. 2010; Fuhrmann, Chini, Kaderhandt & Chen 2017; Moe & Di Stefano 2017; Moe 2019), while for massive stars, the fraction reaches 100% (Sana et al. 2014)

More recently, Moe, Kratter & Badenes (2019) showed that the close binary fraction of solar-type stars is strongly anti-correlated with metallicity, varying from 0.53±0.12 at [Fe/H]=−3 to 0.10±0.03 at [Fe/H]=+0.5 (see also Gao et al. 2017).

Fewer studies have looked at the mass-ratio distribution as a function of the primary mass, although there is a general trend for them to be compatible with a flat distribution in a wide range of parameter (see the refs. cited above, as well as, e.g., Gullikson, Kraus & Dodson-Robinson 2016; Shahaf & Mazeh 2019). Here we want to see if we can use *Gaia* DR2 to quantify this further.

2. Creating the sample

Following up on the work of Boffin & Pourbaix (2018), we aim here at determining the mass ratio distributions of spectroscopic binary systems as a function of the mass of the primary. To this aim, we use the SB9 catalogue (http://sb9.astro.ulb.ac.be; Pourbaix et al.

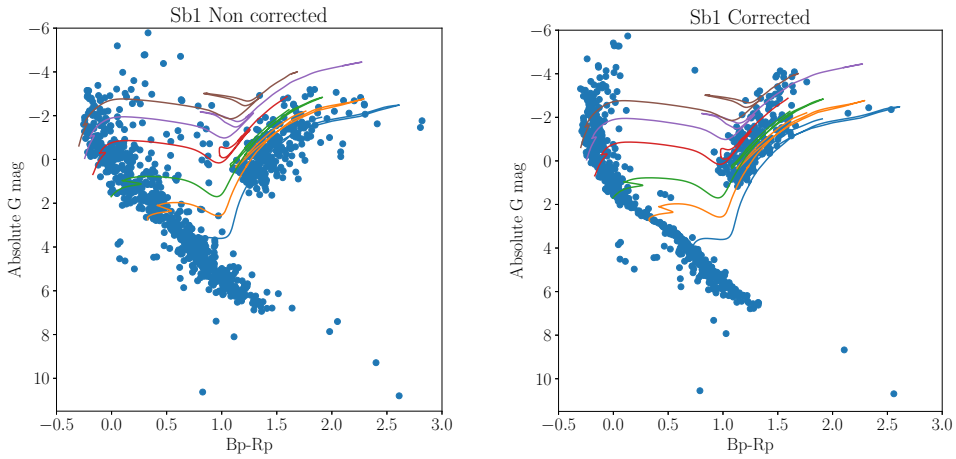

Fig. 1. *Gaia* colour-magnitude diagram for the SB1 of our sample, without any correction for the interstellar extinction (left) and with (right). BASTI theoretical tracks for 1, 2, 3, 4, and 5 $M_{\odot}$ stars are also indicated. The correction makes the main-sequence much narrower and brings the red giants to positions compatible with the tracks.

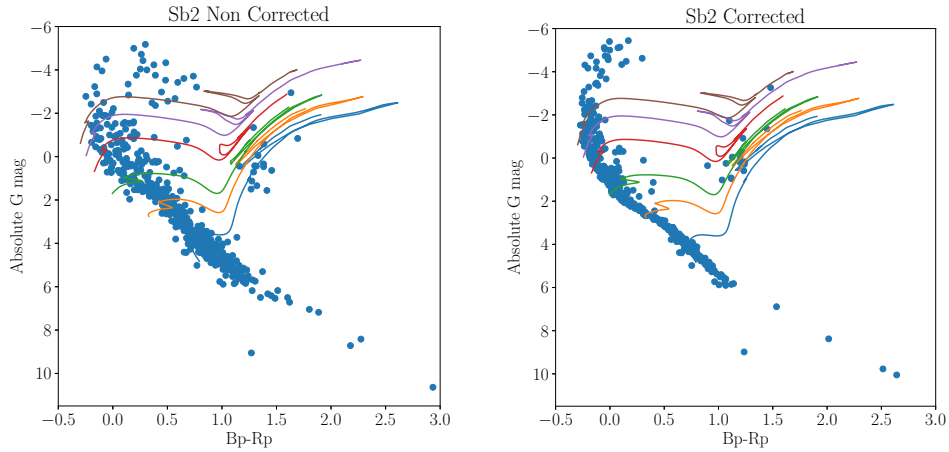

Fig. 2. *Gaia* colour-magnitude diagram for the SB2 of our sample, without any correction for the interstellar extinction (left) and with (right).

2004), which is an online catalogue of spectroscopic orbits that was setup in 2003 and is regularly updated. The current version of the catalogue contains 3814 systems, more than twice as many as in its previous release (Batten, Fletcher & MacCarthy 1989), which contained 1469 systems. Only 3094 systems are cross matched with 3009 distinct *Gaia* DR2 source ids. Among these *Gaia* entries, 2016 are single-lined spectroscopic binaries (SB1) and 1078 are double-lined (SB2).

We then cross-correlated the SB9 catalogue with *Gaia* DR2 (Gaia Collaboration et al. 2016, 2018), keeping only those systems

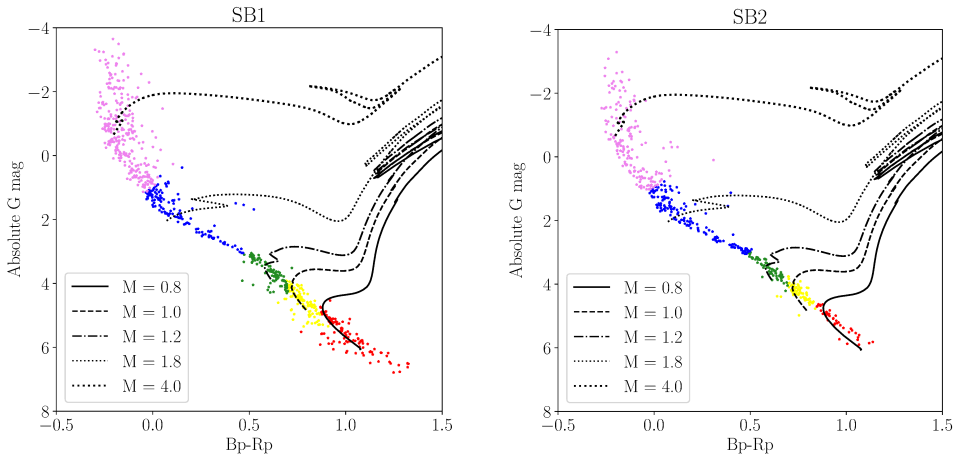

Fig. 3. The final *Gaia* colour-magnitude diagram for all the main-sequence stars in our samples: SB1 (left) and SB2 (right). We also indicate the boundaries between the various spectral types as used in this paper.

for which *Gaia* provided a measurement of the extinction in the G-band (A_g) and for which the *Gaia* parallax (ϖ) had a relative error below 10%. The latter constraint is used to ensure that the distance is well known and the error on the absolute magnitude is also sufficiently constrained (remembering that the error on the absolute magnitude is slightly more than twice as big as the relative error on the parallax). The need for a measured A_g stems from the fact that we need to put the stars in a colour-magnitude diagram and ignoring extinction can have a dramatic effect. This is clearly demonstrated in Figs. 1 and 2. These figures are colour-magnitude diagrams (i.e. plotting the absolute G magnitude vs. the colour $B_p - R_p$), where we also show the position of the BASTI isochrones (`http://basti-iac.oa-abruzzo.inaf.it/tracks.html`; Hidalgo et al. 2018). It is obvious from Fig. 1 that including the extinction allows to narrow very much the main sequence as well as to bring all the red giants in the expected location. This is thus critical to have a good estimate of the primary mass (M_1). The effect is also clear in Fig. 2, although as expected the number of red giants in this sub-sample is much smaller – this is a direct consequence of the fact that a SB2 with a red giant primary requires a red giant companion, which in turn will only happen for a mass ratio very close to 1 (i.e. twins).

Table 1. Numbers of systems considered

Systems	Total	A_g	$\frac{\sigma_\varpi}{\varpi} < 10$	MS
SB1	2016	1143	1067	738
SB2	1078	567	534	488

Finally, we have selected from the colour-magnitude diagrams (CMD) only those stars that are on the main sequence. The final set of systems we have selected is indicated in Tab. 1. Interpolating from the BASTI set of evolutionary tracks, we associated to each primary in our systems a mass. The resulting, final CMDs are shown in Fig. 3, where we also indicate very roughly the spectral type associated to each systems, as our final aim is to determine the mass ratio as a function of the primary spectral type. For SB2s, our determination of the primary mass will obviously be influenced by the presence of the companion (which, by definition, contributes to the light in the system), which moves the position of the system in the CMD, with respect to a single

Table 2. Distribution in spectral types

Spectral Type	Number SB1	Number SB2	$< M_1 >$ ($M_\odot$)
K	116	41	0.74 ± 0.06
G	117	67	0.95 ± 0.05
F	99	65	1.18 ± 0.08
A	131	151	1.81 ± 0.28
B	275	164	3.82 ± 1.18

star. We have, however, verified that the effect is sufficiently small that it will not move a star from one spectral type to another – instead it generally implies that a system appears slightly more evolved than a single star, but of the same mass. The final number of systems we used in each spectral type is indicated in Tab. 2.

3. Mass ratio distributions

For SB2, deriving the mass ratio distribution for each sub-sample is a trivial thing, as per definition, the mass ratio is obtained from the radial-velocity curves of both components. The resulting values, as a function of the primary mass is shown in Fig. 4, where it can be seen that the mean mass ratio is only very slightly dependent on the primary mass and is, as expected, between 0.7 and 0.8.

In the case of SB1 systems, things are more complicated, as the only observable we have is the spectroscopic mass function:

$$f(m) = \frac{K_1^3 P}{2\pi G}(1-e^2)^{3/2} \equiv \frac{(M_2 \sin i)^3}{(M_1+M_2)^2}, \qquad (1)$$

where K_1 is the semi-amplitude of the radial velocity curve, P is the orbital period, e, the eccentricity, G, the gravitational constant, and M_1 and M_2 are the masses of the primary and secondary. As M_1 is determined from the CMD, we have

$$\frac{f(m)}{M_1} = \frac{(q \sin i)^3}{(1+q)^2}, \qquad (2)$$

where q is the mass ratio. As M_1 is known, we can thus obtain the distribution of $\frac{f(m)}{M_1}$ and, using a de-convolution method that assumes that i is randomly distributed on the sky (Boffin, Paulus & Cerf 1992; Mazeh & Goldberg 1992; Boffin 2010; Shahaf, Mazeh & Faigler 2017), we can thereby derive the **distribution** of the mass ratio, q. The distributions so obtained for SB1 and SB2 systems are shown in the left panel of Fig. 5, where one can see that they complement each other. One can then add the distributions of mass ratio obtained for SB1 and SB2 to derive the final mass ratio distribution, as shown in the same figure.

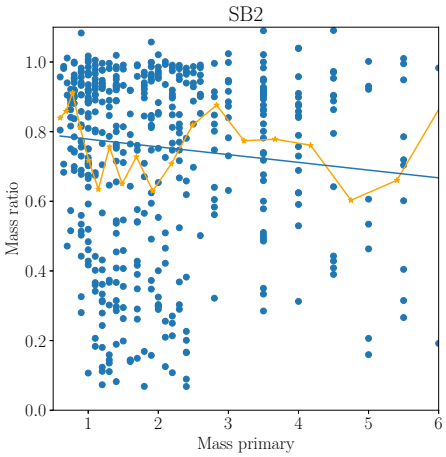

Fig. 4. The mass ratio as a function of the primary mass for all the SB2 in our sample. The original line is the binned mean of the mass ratios, and the blue line is a linear fit to this mean.

As we are interested in obtaining the initial mass ratio distributions as a function of primary mass, we would like as much as possible to not include in our sample post-mass transfer systems, which are characterised by smaller eccentricities and have white dwarf companions (e.g., Van der Swaelmen et al. 2017; Murphy et al. 2018). As this is not easy to implement, as a first step we excluded from our sample all systems which show a circular orbit as, except for some short period systems, this is generally due to mass transfer. The resulting mass ratio distribution (MRD) is shown in the right panel of Fig. 5. The overall shape of the MRD does not change much, except perhaps for a smaller contribution of twins. The

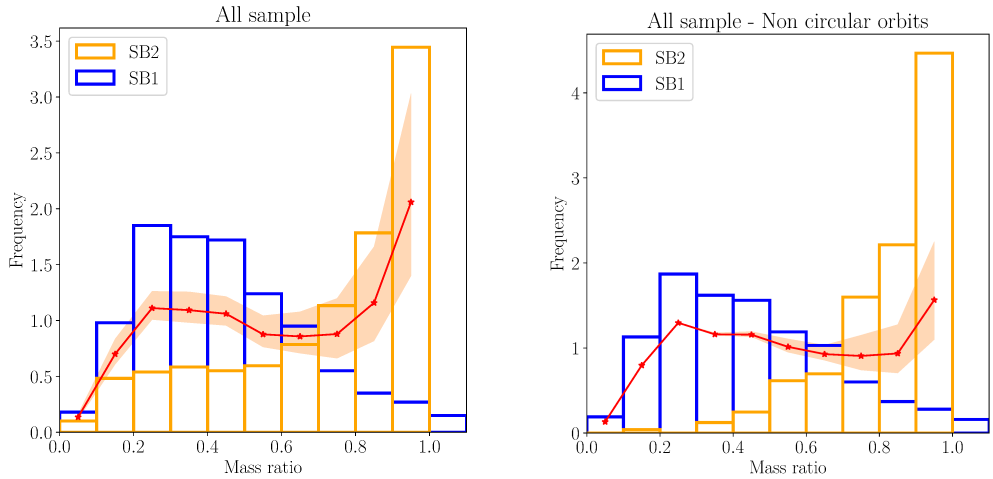

Fig. 5. The mass ratio distributions for SB1 (blue histogram) and for SB2 (orange histogram) for the whole sample (left) and for the eccentric systems (right). The red line is the weighted sum of both distributions, with the shaded regions indicating the range where one assumes that 50% to 150% of all SB2 should be considered in the sum.

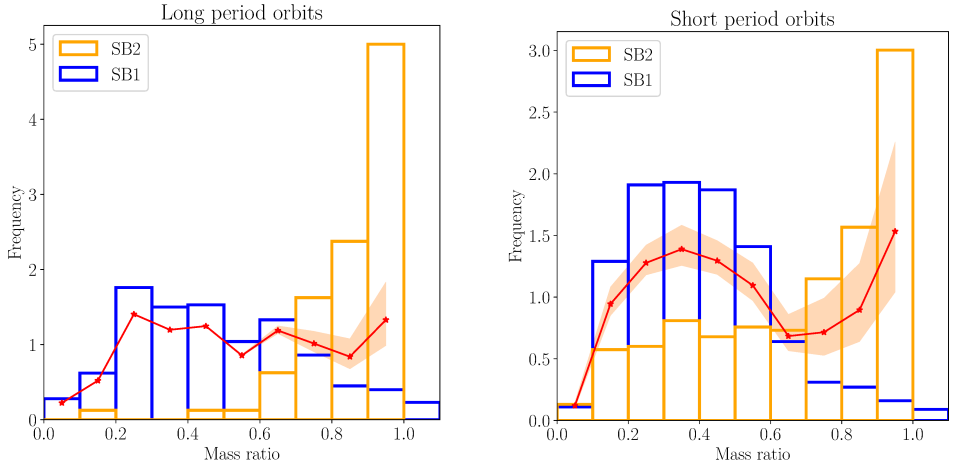

Fig. 6. Same as Fig. 5 when splitting the sample between long-period orbits ($P > 50$ d; left) and short-period orbits.

MRD of this sample is basically uniform between $q = 0.2$ to 0.8, with a lack of the smaller mass ratios and an excess of larger mass ratios.

In order to find the possible origin of the excess, we further split our sample into short-period orbits ($P < 50$ d) and long-period orbits. The resulting MRDs are shown in Fig. 6. It can be seen that for long-period systems, the excess of twins disappeared and the overall distribution is compatible with a uniform distribu-

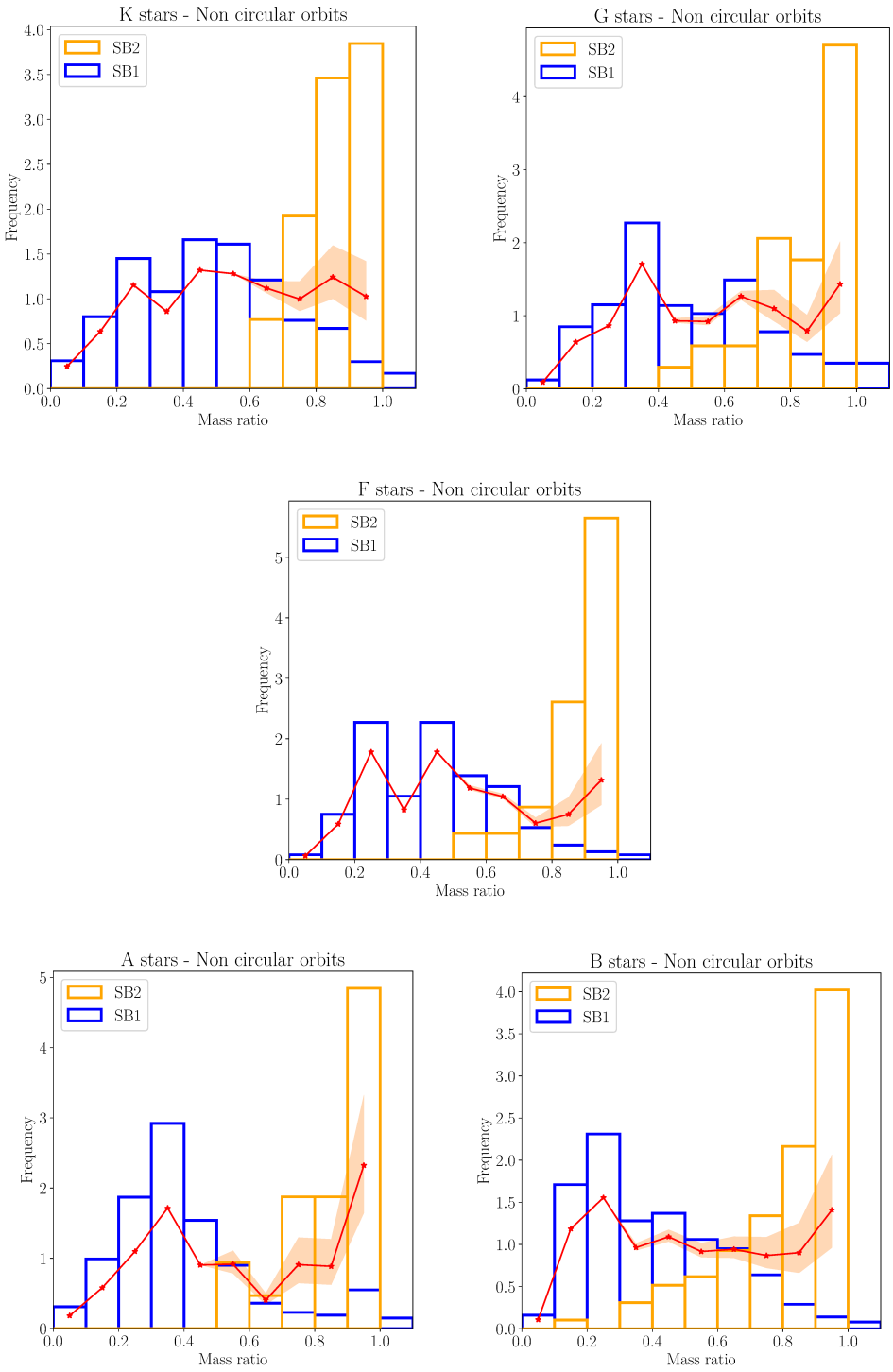

Fig. 7. Same as Fig. 5 for the eccentric systems, split among the spectral types.

tion, at least for $q > 0.2$. This confirms a result already found by Halbwachs et al. (2003) for solar-type stars.

We can now derive the MRDs for the subsamples corresponding to each spectral type. This is shown in Fig. 7. The MRDs of the various spectral types seem to indicate some differences. Thus, A stars seem to show a bimodal distribution, peaked at $q = 0.3$ and $q = 0.9$, while B stars have more low-mass companions. Our results should provide useful constraints to models of star formation.

Acknowledgements. D.P is a Senior FNRS Research Associate. This work has made use of data from the European Space Agency (ESA) mission *Gaia* (`https://www.cosmos.esa.int/gaia`), processed by the *Gaia* Data Processing and Analysis Consortium (DPAC, `https://www.cosmos.esa.int/web/gaia/dpac/consortium`). Funding for the DPAC has been provided by national institutions, in particular the institutions participating in the *Gaia* Multilateral Agreement.

References

Batten, A. H., Fletcher, J. M., MacCarthy, D. G. 1989, Publ. Dom. Astrophys. Obs. Victoria, 17, 1

Boffin, H. M. J. 2010, A&A, 524, A14

Boffin, H. M. J., Paulus, G., Cerf, N. 1992, in Binaries as Tracers of Star Formation, ed. A. Duquennoy and M. Mayor (Cambridge Univ. press, Cambridge), 26

Boffin, H. M. J., Pourbaix, D. 2018, in Astrometry and Astrophysics in the *Gaia* Sky, ed. A. Recio-Blanco, et al. (Cambridge Univ. Press, Cambridge), IAU Symp., 330, 339

Duchêne, G., Kraus, A. 2013, ARA&A, 51, 269

Duquennoy, A., Mayor, M. 1991, A&A, 500, 337

Fuhrmann, K., Chini, R., Kaderhandt, L., Chen, Z. 2017, ApJ, 836, 139

Gaia Collaboration, Prusti, T., de Bruijne, J. H. J., et al. 2016, A&A, 595, A1

Gaia Collaboration, Brown, A. G. A., Vallenari, A., et al. 2018, A&A, 616, A1

Gao, S., Zhao, H., Yang, H., Gao, R. 2017, MNRAS, 469, L68

Gullikson, K., Kraus, A., Dodson-Robinson, S. 2016, AJ, 152, 40

Halbwachs, J. L., et al. 2003, A&A, 397, 159

Hidalgo, S. L., et al. 2018, ApJ, 856, 125

Mazeh, T., Goldberg, D. 1992, ApJ, 394, 592

Moe, M., in The Impact of Binary Stars on Stellar Evolution, ed. G. Beccari and H.M.J. Boffin (Cambridge Univ. Press, Cambridge), Cambridge Astrophys. Series, 54, 12

Moe, M., Di Stefano, R. 2017, ApJS, 230, 15

Moe M., Kratter, K. M., Badenes, C. 2019, ApJ, 875, 61

Murphy, S. J., et al. 2018, MNRAS, 474, 4322

Pourbaix, D., et al. 2004, A&A, 424, 727

Raghavan, D., et al. 2010, ApJS, 190, 1

Sana, H., et al. 2014, ApJS, 215, 15

Shahaf, S., Mazeh, T., Faigler, S. 2017, MNRAS, 472, 4497

Shahaf, S., Mazeh, T. 2019, MNRAS, 487, 3356

Van der Swaelmen, M., et al. 2017, A&A, 597, A68

Ward-Duong, K., et al. 2015, MNRAS, 449, 2618